TOWARDS A LARGE TIMESTEP ALGORITHM FOR SYSTEMS OF CONSERVATION LAWS: PRELIMINARY RESULTS IGNORING INTERACTIONS

R. J. LEVEQUE

Numerical Analysis report 9/82

Dept. of Mathematics
University of Reading

Author's current address:

New York University
Courant Institute of Mathematical Sciences
251 Mercer Street
New York, NY 10012

This research was supported by a National Science Foundation postdoctoral fellowship.

1. Introduction.

In [2] a large timestep generalization of Godunov's method was proposed for solving scalar conservation laws in one space dimension. The use of larger timesteps results in considerably less smearing of discontinuities. In Godunov's method each jump discontinuity $u^n_{j+1} - u^n_j$ is propagated according to the Rankine-Hugoniot jump condition to its proper location at time t_{n+1}. The resulting solution is then averaged over intervals $[x_{j-1/2}, x_{j+1/2}]$ to give u^{n+1}_j. The usual Courant number restiriction for Godunov's method ensures that the discontinuities do not interact with one another over the course of a single timestep.

In the large timestep generalization, discontinuities are allowed to propagate through several mesh points in each timestep. In general the discontinuities should then interact with one another. In practice we can either attempt to recognize and handle these interactions or we can ignore them. The former approach is clearly superior and for scalar problems it was found that this could be done easily and efficiently through a merging procedure. Unfortunately, that procedure does not generalize dirctly to systems and it is doubtful whether any such procedure exists that is sufficiently efficient to allow us to handle all interactions correctly. The question then arises as to whether most interactions in a typical problem can be ignored in each timestep, perhaps concentrating our effort on handling interactions between strong discontinuities.

As a first step in this direction it is useful to experiment with the method in which all interactions are ignored, in order to see where difficulties arise. This has been done for a simple model problem and some results are reported on here. It is found that in smooth regions of the flow it may be quite reasonable to ignore interactions, at least with moderate timesteps. Moreover, shock propagation and interactions are handled remarkably well in some cases, often giving sharp and accurate results, although these results are highly variable and depend strongly on both the Courant number and the meshsize used.

An interesting phenomenon is observed in which gross inaccuracies in the solution caused by incorrectly handling interactions at one timestep will often be corrected in later timesteps. This gives further hope that a more sophisticated algorithm, in which the most important interactions are handled explicitly, will indeed be able to deal with realistic problems successfully and efficiently.

2. Numerical results.

Computations have been performed only on a model system of two equations obtained by setting $\gamma = 1$ in the Euler equations (see Roe[4]). The equations are

$$\begin{aligned} \rho_t + m_x &= 0 \\ m_t + (m^2/\rho + a^2\rho)_x &= 0 \end{aligned} \tag{1}$$

where ρ is the density, m is the momentum, and a is the (constant) sound speed. The eigenvalues of the Jacobian are $m/\rho \pm a$. For simplicity of description we assume that the flow is subsonic everywhere, $|m/\rho| < a$, so that the general solution to a Riemann problem consists of one leftward moving wave and one rightward moving wave, each of which is either a shock or a centered rarefaction wave. The intermediate states and propagation speeds are easily computed for this example. The set of states (ρ, m) which can be connected to a given state (ρ_0, m_0) through a shock satisfy

$$m = \frac{\rho m_0}{\rho_0} \pm a\sqrt{\frac{\rho}{\rho_0}}\,(\rho - \rho_0),$$

the + and − signs corresponding to rightward and leftward moving shocks respectively. The velocity at which a shock propagates is $(m - m_0)/(\rho - \rho_0)$. The set of states which can be connected through a centered rarefaction wave satisfy

$$m = \frac{\rho m_0}{\rho_0} \pm a\rho \ln(\rho/\rho_0).$$

The large timestep algorithm is best described by considering a typical step. We begin by initializing $u_j^{n+1} = u_j^n$ for all j. Now consider a single Riemann problem between x_j and x_{j+1}. Suppose it has been determined that the states u_j^n and u_{j+1}^n are connected through a leftward moving rarefaction wave, an intermediate state u_m, and a rightward moving shock. The intermediate state u_m is obtained by solving for ρ_m and m_m from

$$m_m = \frac{\rho_m m_j}{\rho_j} - a\rho_m \ln(\rho_m/\rho_j)$$

and

$$m_m = \frac{\rho_m m_{j+1}}{\rho_{j+1}} + a\sqrt{\frac{\rho_m}{\rho_{j+1}}}\,(\rho_m - \rho_{j+1}).$$

The discontinuity $u_m - u_{j+1}^n$ propagates to the right with speed

$$c = \frac{m_{j+1} - m_m}{\rho_{j+1} - \rho_m}.$$

Setting $\mu = \lfloor ck/h \rfloor$, the integer part of the speed times the mesh ratio, we increment the values $u_{j+1}^{n+1}, u_{j+2}^{n+1}, \ldots, u_{j+\mu}^{n+1}$ by $u_m - u_{j+1}^n$ and increment $u_{j+\mu+1}^{n+1}$ by $(ck/h - \mu)(u_m - u_{j+1}^n)$. This is equivalent to propagating the discontinuity to the point $x_{j+1/2} + ck$ and projecting the resulting solution on to the grid by averaging, as in Godunov's method. if the Courant number is less than 1 then $\mu = 0$ and only the value u_{j+1}^{n+1} is affected.

Following [2], the rarefaction is split into several weaker discontinuities which are propagated as entropy-violating shocks. This allows the original discontinuity to spread out over several mesh points and gives a good approximation to the true rarefaction wave provided it is split into sufficiently many pieces. Specifically, we take i_r pieces where i_r is some integer roughly proportional to

$$\frac{k}{h}\left|\frac{m_m}{\rho_m} - \frac{m_j}{\rho_j}\right|,$$

the number of grid points the rarefaction wave is spread over at time t_{n+1}. These discontinuities propagate at different velocities and are separated by intermediate states $u_{j,i}$ for $i = 1, 2, \ldots, i_r - 1$ which are given by

$$\rho_{j,i} = \rho_j^n + \frac{i}{i_r}(\rho_m - \rho_j^n)$$

$$m_{j,i} = \frac{\rho_{j,i} m_{j,i-1}}{\rho_{j,i-1}} - a\rho_{j,i} \ln(\rho_{j,i}/\rho_{j,i-1}).$$

These states are shown in the ρ-m plane for $i_r = 3$ in Fig. 1.

Each discontinuity $u_{j,i} - u_{j,i-1}$ is then propagated to the left with velocity

$$c_i = \frac{m_{j,i} - m_{j,i-1}}{\rho_{j,i} - \rho_{j,i-1}}$$

just as the shock was propagated to the right. This scheme can be shown to be conservative.

As a numerical example, the following initial conditions have been used:

$$u(x,0) = \begin{cases} u_1, & 0 \le x < 0.1, \\ u_2, & 0.1 \le x < 0.5, \\ u_4, & 0.5 \le x < 0.98, \\ u_5, & 0.98 \le x \le 1, \end{cases}$$

where

$$u_1 = \begin{bmatrix} 0.5 \\ 0.111803 \end{bmatrix}, \qquad u_2 = \begin{bmatrix} 0.4 \\ 0 \end{bmatrix}, \qquad u_4 = \begin{bmatrix} 0.2 \\ 0 \end{bmatrix}, \qquad u_5 = \begin{bmatrix} 0.35 \\ -0.19843 \end{bmatrix}.$$

We take $a = 1$. The states u_1 and u_2 are separated by a shock moving to the right, u_4 and u_5 by a shock moving to the left. The states u_2 and u_4 are separted by a rarefaction moving to the left, an intermediate state

$$u_3 = \begin{bmatrix} 0.28260 \\ 0.098185 \end{bmatrix},$$

and a shock moving to the right. We compare computed and exact solutions at time 0.16, before any interaction has occured, and at time 0.32, after the shock separating u_1 and u_2 has interacted with the rarefaction separating u_2 and u_3 and the two shocks in the right half of the interval have also interacted (see Fig. 2).

For this problem the Courant number is roughly $\nu \approx 1.5\lambda$, where $\lambda = k/h$. Figures 3 and 4 show computations with $h = 1/50$ and various values of λ. For $\lambda = 0.5$, $\nu < 1$ and we have Godunov's method. Note the excesssive smearing of shocks. Taking $\lambda = 1$ gives a dramatic improvement. Another slight improvement is seen in going to $\lambda = 2$. For $\lambda = 4$ and 8 the results at $t = 0.16$ continue to improve but the interactions are handled poorly and the results at $t = 0.32$ are completely incorrect in some regions.

The same computations with $h = 1/100$ reveal an interesting phenomenon. With this smaller value of h the results with $\lambda = 4$ (Fig. 5a,b) are much better while the results for $\lambda = 8$ (Fig. 5c,d) have also improved and now look very similar to the previous results with $\lambda = 4$.

This will be explained in the next section, where we will see that errors caused by ignoring interactions tend to correct themselves in later timesteps, so that in this simple problem the accuracy is determined in part by the number of steps taken since the interaction. Since with fixed λ reducing the timestep increases the number of steps taken since the interaction, and thus increases the amount of "self-correction" which has taken place, a substantial improvement in the solution is seen.

This argument is valid in the right half of the intervaal, where only a single interaction takes place in the true solution, but comparing Figures 4b and 5b shows that the shock-rarefaction interaction is also handled more successfully, even though in this region new interactions occur (and are incorrectly handled) in every timestep.

Smooth solutions. As another test of the algorithm we have made a more quantitative comparison of the accuracy obtained with different Courant numbers on smooth solutions. The initial conditions used are

$$\rho(x,0) = 0.2 + 0.3\exp(-10(x-0.5)^2)$$
$$m(x,0) = -0.1\sin(2\pi x)$$

TABLE 1

Max norm of errors in smooth solution at $t = 0.08$. Errors in ρ and m are shown.

	$h = 1/25$	$h = 1/50$	$h = 1/100$
$\lambda = 0.5$	7.831(-3)	4.479(-3)	2.118(-3)
	4.062(-3)	2.118(-3)	8.485(-4)
$\lambda = 1.0$	6.676(-3)	3.531(-3)	1.259(-3)
	5.157(-3)	2.819(-3)	1.047(-3)
$\lambda = 2.0$	7.041(-3)	3.836(-3)	1.402(-3)
	4.803(-3)	2.392(-3)	8.598(-4)
$\lambda = 4.0$		4.575(-3)	1.743(-3)
		3.436(-3)	1.291(-3)

for which the Courant number is again roughly $\nu \approx 1.5\lambda$. The errors at time $t = 0.08$ are shown in Table 1. These show that for Courant numbers larger than 1 the method remains first order accurate. Moreover, in many cases the results obtained with large Courant numbers are in fact better than those obtained with smaller values. Some explanation of this will also be given in the next section.

These positive numberical results lead to the conjecture that the results obtained by the algorithm described here converge to the true solution as $k, h \to 0$ for any fixed value of the Courant number.

3. Analysis.

First consider the effect of applying this algorithm to a linear system

$$u_t + Au_x = 0$$

where A is a constant $N \times N$ matrix. Each discontinuity $u^n_{j+1} - u^n_j$ is decomposed as

$$u^n_{j+1} - u^n_j = e^{(1)}_j + e^{(2)}_j + \cdots + e^{(N)}_j$$

where the $e^{(i)}_j$ are eigenvectors of A. The discontinuity $e^{(i)}_j$ then propagates at a speed given by the corresponding eigenvalue μ_i. If the Courant number $\frac{k}{h} \max |\mu_i|$ is greater than 1 then discontinuities from neighboring Riemann problems are again allowed to simply pass through one another.

For the linear problem, ignoring interactions in this manner is in fact the correct way to handle them, and (except for the projection process) the exact solution is obtained after a single timestep of any length.

To see that this is so, write the true solution $u(x,t)$ as

$$u(x,t) = r^{(1)}(x,t) + \cdots + r^{(N)}(x,t)$$

where the $r^{(i)}(x,t)$ are eigenvectors of A. Then the true solution at time $t+k$ is given by

$$u(x,t+k) = r^{(1)}(x-\mu_1 k, t) + \cdots + r^{(N)}(x-\mu_N k, t).$$

In other words,

$$r^{(i)}(x,t+k) = r^{(i)}(x-\mu_i k, t).$$

We will decompose the numerical approximation in the same manner,

$$u_j^n = r_j^{(1)n} + \cdots + r_j^{(N)n}.$$

Since our algorithm handles each eigenvector separately, it is sufficient to look at a single eigenvector, say $r^{(i)}$. For concreteness suppose $\mu_i > 0$ and set $\mu = \lfloor \mu_i k/h \rfloor$. Then from each grid point x_j the jump $e_j^{(i)}$ in the ith eigenvector propagates through μ mesh points, and part way through another. Turning this around and looking at what increments a fixed grid point receives when the algorithm is applied everywhere we find that

$$\begin{aligned} r_j^{(i)n} &= r_j^{(i)n} - e_{j-1}^{(i)} - e_{j-2}^{(i)} - \cdots - e_{j-\mu}^{(i)} - (\mu_i \tfrac{k}{h} - \mu) e_{j-\mu-1}^{(i)} \\ &= (1 - (\mu_i \tfrac{k}{h} - \mu)) r_{j-\mu}^{(i)n} + (\mu_i \tfrac{k}{h} \mu) r_{j-\mu-1}^{(i)n}. \end{aligned}$$

So $r_j^{(i)n+1}$ is obtained by linearly interpolating between $r_{j-\mu}^{(i)n}$ and $r_{j-\mu-1}^{(i)n}$ and hence is an $O(h^2)$ approximation to $r^{(i)}(x-\mu_i k, t)$. This is true for each of the eigenvectors and so the algorithm is simply the method of characteristics with linear interpolation.

For linear problems the only error is due to the projection (i.e. interpolation) process and so it is best to take very large timesteps, thus reducing the number of interpolations performed.

This behavior on the linear problem gives some indication of why the large timestep algorithm computes smooth solutions to nonlinear problems as well as it does. In a smooth solution the eigenvectors are locally nearly constant and the characteristics are nearly straight lines. There is a tradeoff between reducing the errors due to the nonlinearity by taking λ small, and reducing the errors due to interpolation by taking λ large. The optimal λ will depend on the deviation from linearity.

Shock interactions. In order to analyze the manner in which the algorithm handles shock interactions we return to the linear problem and view interactions there from a different standpoint. Consider a system with 2 variables which we again denote by ρ and m. Take initial conditions with two discontinuities:

$$u(x,0) = \begin{cases} u_1, & x < x_1, \\ u_3, & x_1 < x < x_2, \\ u_5, & x_2 < x. \end{cases}$$

The true solution is shown in Fig. 6.

If the u_j are decomposed into eigenvectors $r_j^{(1)}, r_j^{(2)}$ corresponding to the eigenvalues $\mu_1 < \mu_2$,

$$u_1 = r_1^{(1)} + r_1^{(2)},$$
$$u_3 = r_3^{(1)} + r_3^{(2)},$$
$$u_5 = r_5^{(1)} + r_5^{(2)},$$

then the intermediate states u_2, u_4 and $\tilde{u}_3$ are given by

$$u_2 = r_3^{(1)} + r_1^{(2)},$$
$$u_4 = r_5^{(1)} + r_3^{(2)},$$
$$\tilde{u}_3 = r_5^{(1)} + r_1^{(2)}.$$

The fact that the interaction is handled correctly is a consequence of the fact that

$$\tilde{u}_3 = u_3 - (u_3 - u_2) + (u_4 - u_3),$$

the latter two quantities being the increments u_3 receives in the overlap region after propagating the discontinuities. Fig. 7 shows these states in the ρ-m plane. Adjacent states are connected by eigenvectors.

The fact that $\tilde{u}_3 = u_2 + u_4 - u_3$ will be expressed by saying that $\tilde{u}_3$ is the *linear reflection* of u_3 through the collision of u_2 and u_4.

For the nonlinear problem with similar initial conditions the solution is shown in Fig. 8 (for convenience we take $u_1 = u_2$ and $u_4 = u_5$). This corresponds to Fig 9 in the ρ-m plane.

Because of the nonlinearity, the shock speeds change after the collision of u_2 and u_4 and the state $\tilde{u}_3$ is no longer the linear reflection of u_3. The large timestep algorithm, by propagating the discontinuities through one another, ignores these facts. After one timestep it produces the solution shown in Fig. 10, where $u_3^* = u_2 + u_4 - u_3$ is the linear reflection of u_3 through u_2 and u_4 as seen in Fig. 11.

The accuracy of the computed solution again depends on the deviation from linearity as well as the strength of the shocks involved.

The self-correction phenomenon alluded to earlier can now be explained. Consider the next timestep, from $t + k$ to $t + 2k$. Each of the discontinuities present give rise to two new waves, separated by new intermediate states u_5 and u_6. When states u_5 and u_6 collide a new state u_3^{**} appears which is the linear reflection of u_3^*. This is shown in Fig. 12 together with the true solution from Fig. 8 as a dotted line.

From Fig. 13 it is clear that u_3^{**} is much closer to the true state $\tilde{u}_3$ than was u_3^*. (In Fig. 4b one can clearly see the states u_5, u_3^{**} and u_6 in the shock-shock interaction.)

Further correction-waves are generated in later steps, pushing the intermediate state even closer to $\tilde{u}_3$ and restoring the outer shocks to their correct trajectories.

4. Conclusions.

We are still left with the problem of identifying which interactions must be handled explicitly in a given computation and the task of devising an efficient algorithm to do so. This is necessary if dependable results are to be generated using truly large timesteps.

On the other hand, it may prove better to restrict our attention to moderate values of the Courant number, say $\nu = 2$ or 3, and ignore interactions. For such values of ν incorrect intermediate states will be confined to a few mesh points. If these inaccuracies

are quickly corrected in subsequent timesteps this may be a reasonable algorithm. Our goal of maintaining sharp shocks will be at least partly accomplished since the numerical results indicate that the most dramatic improvement in the solution occurs in going from $\nu < 1$ to $\nu \approx 1.5$.

Several further comments should be made about the results presented here and possible directions for future research.

Even ignoring interactions between shocks of different characteristic families, the propagation of an isolated shock can already lead to difficulties. The results presented here may give a false impression as to the ease with which this is handled. In general the shock is smeared over at least two intervals in order to represent it on the fixed grid. The intermediate state introduced in this manner is a convex combination of the left and right states, and in general will not lie on the Hugoniot curve between those states. In the next timestep each of the resulting discontinuities will generate waves of both characteristic families. The ones going backwards apparently cancel one another out. (The numerical evidence for this is supported by considering their positions in the phase plane.) Of the waves moving forward, the trailing shock travels faster than the leading shock and, for large Courant numbers, may end up several grid points in front, causing an unphysical smearing of the shock (see Fig. 4.1 in [2]). This has not happened in our examples because of the small relative difference in shock velocities (due to our choice of a subsonic example) and because only moderate values of the Courant number have been considered.

Further difficulties may appear when this method is applied to the full Euler equations, particularly in handling contact discontinuities. One expects that contact discontinuities will still tend to smear over time, lacking the restoring forces of shocks, but that at larger Courant number the smearing will proceed more slowly due to the reduction in the number of steps and hence the number of projections it undergoes. It is not clear how well interactions involving contact discontinuities will be handled.

Many of the difficulties stemming from averaging the solution at each timestep may be best avoided by eliminating the fixed grid altogether and representing the solution at each time by a list of discontinuities and their positions. This is almost certainly the best approach for scalar problems, but for a system of N equations each discontinuity may split into N new discontinuities at every timestep. It will be necessary to merge discontinuities in order to avoid an exponential growth in the amout of information retained.

We note that in general it is impossible to merge two discontinuities into a single discontinuity in a conservative manner but that it is always possible to merge an arbitrary number of discontinuities at points $x_1, x_2, \ldots, x_r$ into two discontinuities at the points x_1 and x_r. The correct intermediate state is obtained simply by averaging the original solution (i.e. integrating between x_1 and x_r). By ensuring that strong discontinuities always lie at the endpoint of some integration interval it may be possible to avoid a great deal of smearing and many of the associated problems. Harten and Hyman[1] have used a similar approach with good results.

For the model system considered here the exact solution to the Riemann problem was always used, except in rarefaction waves. For practical problems it may be desirable to use approximate Riemann solvers such as those advocated by Roe[3]. Each discontinuity is then split into eigenvectors of some locally defined matrix $\tilde{A}$ which are propagated at velocities given by the corresponding eigenvalues. For the model system (1), Roe[4]

recommends using the matrix

$$\tilde{A}(u_j, u_{j+1}) = \begin{bmatrix} 0 & 1 \\ a^2 - v^2 & 2v \end{bmatrix}$$

where v is the weighted average of velocities

$$v = \frac{m_j^{1/2}/\rho_j^{1/2} + m_{j+1}^{1/2}/\rho_{j+1}^{1/2}}{\rho_j^{1/2} + \rho_{j+1}^{1/2}}.$$

Preliminary numerical results indicate that the use of this approximate Riemann solver leads to some degradation of the solution with large timesteps, but that the method still converges for arbitrary Courant number.

The use of an approximate Riemann solver leads to the calculation of incorrect intermediate states and propagation speeds for each discontinuity at every timestep. This shows up most clearly when larger timesteps are used but it is true in all calculations. It appears that these incorrect states are automatically corrected in later timesteps in much the same way as large timestep interactions are corrected. This suggests a close connection between approximate solutions to the Riemann problem and our approximate handling of interactions.

Acknowledgments. The author would like to express appreciation to the Mathematics Department of the University of Reading for their hospitality. This work has benefitted from discussions with many people there, including M.J. Baines, K.W. Morton, and P.L. Roe of the Royal Aircraft Establishment.

The manuscript was produced using TEX, a computer typesetting system created by Donald Knuth at Stanford.

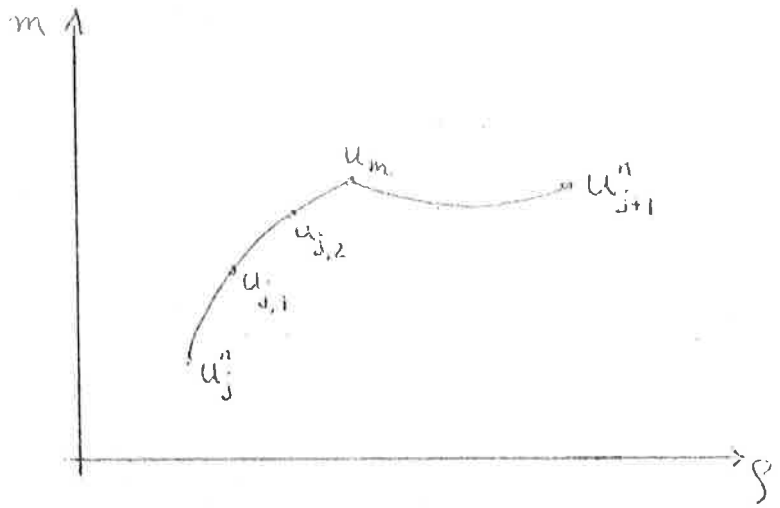

FIG. 1

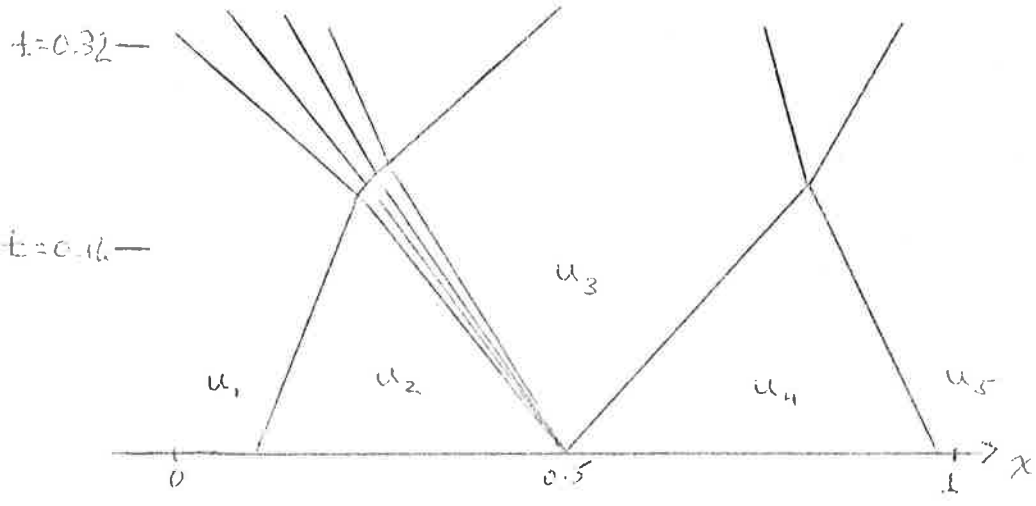

FIG. 2

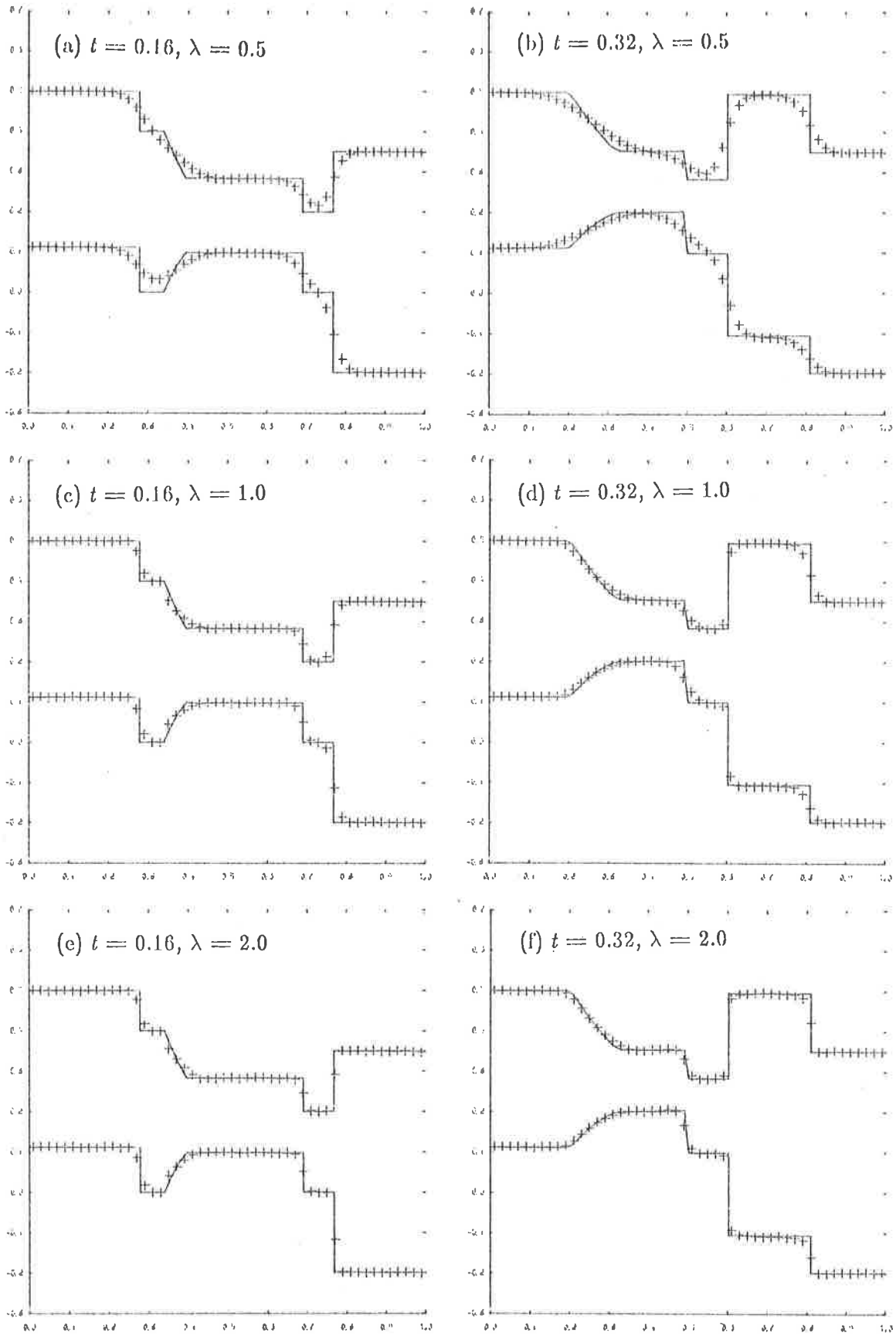

FIG. 3. Solutions ρ and m obtained using 50 mesh points.

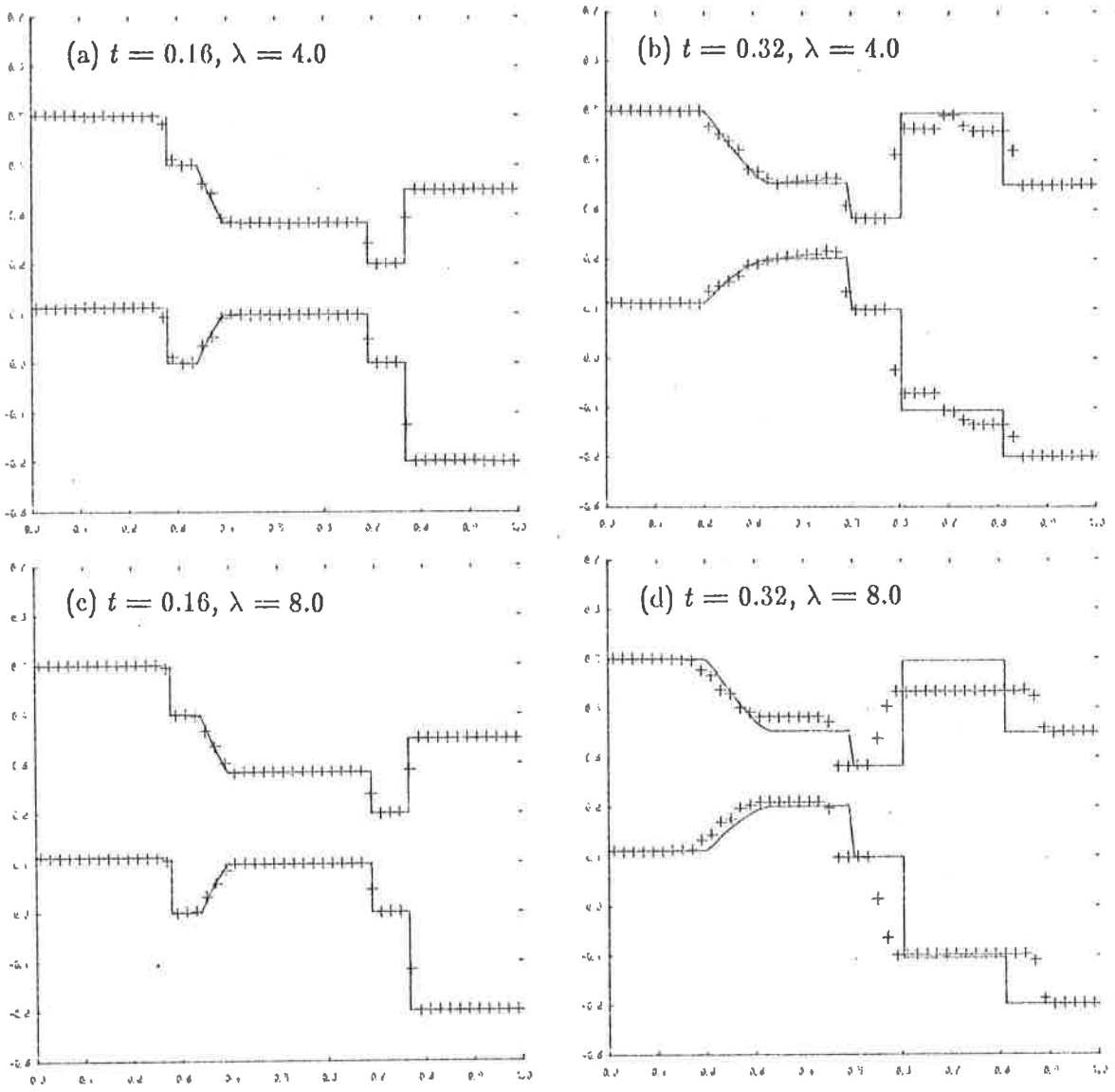

FIG. 1. Solutions ρ and m obtained using 50 mesh points.

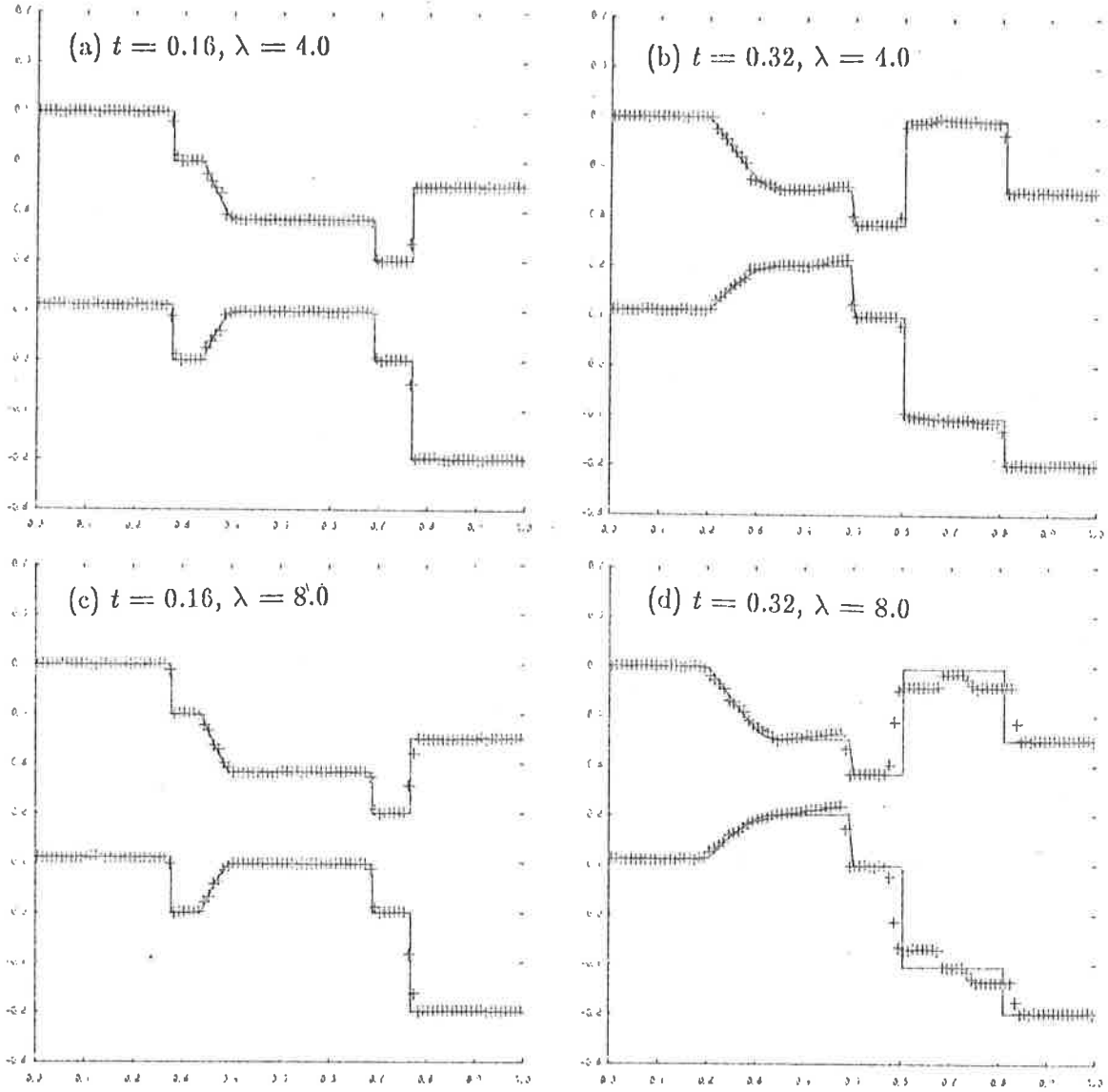

FIG. 5. Solutions ρ and m obtained using 100 mesh points.

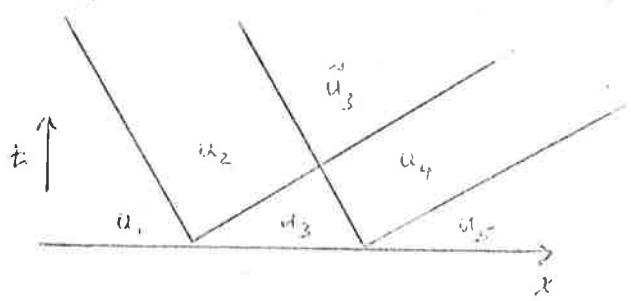

FIG. 6

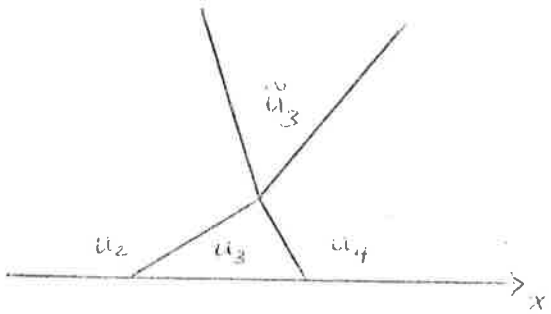

FIG. 8

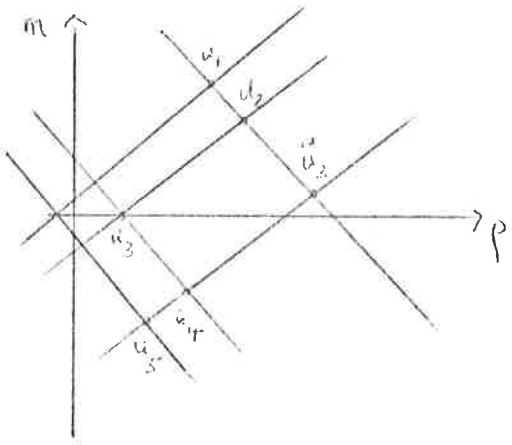

FIG. 7

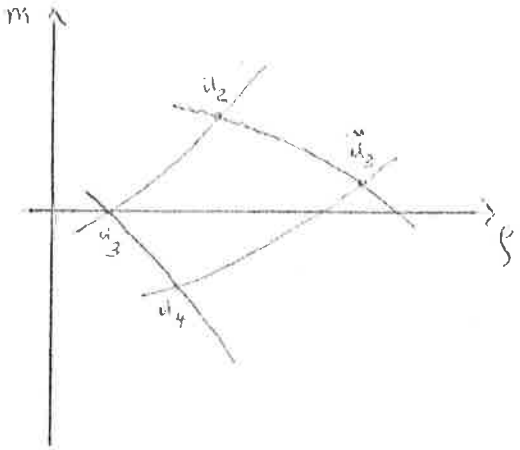

FIG. 9

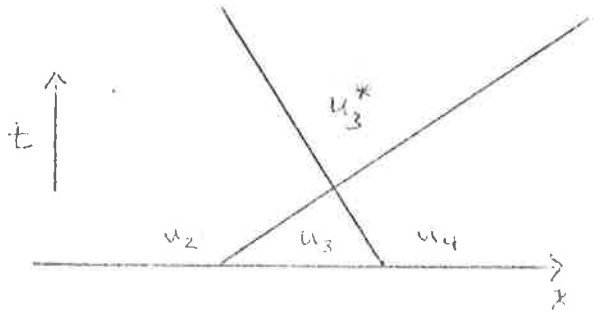

FIG. 10

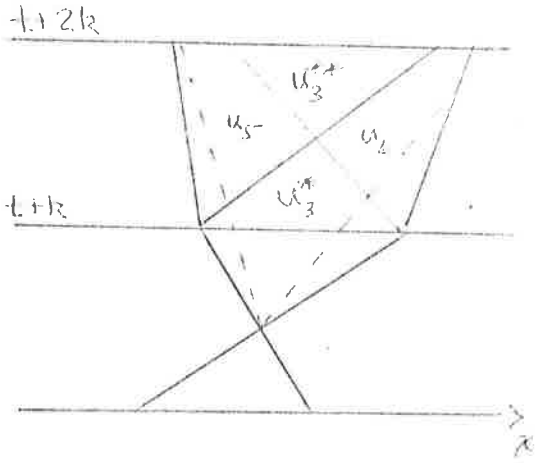

FIG. 12

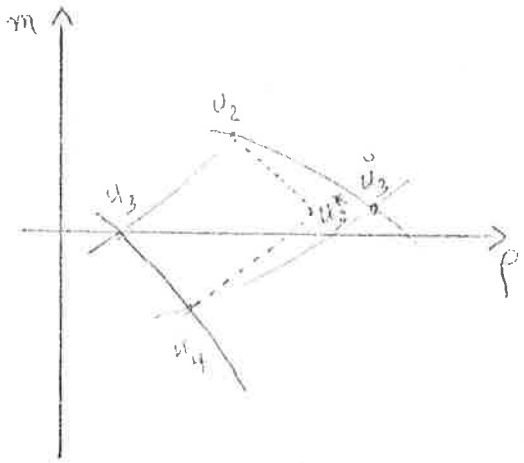

FIG. 11

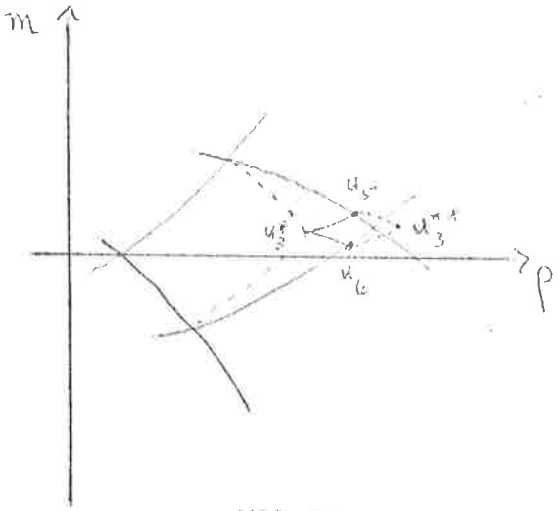

FIG. 13

REFERENCES

[1] A. Harten and J.M. Hyman, A self-adjusting grid for the computation of weak solutions of hyperbolic conservation laws: I. One-dimensional problems, Los Alamos report LA-9105, 1981.

[2] R.J. LeVeque, Large time-step shock capturing techniques for scalar conservation laws, Stanford Numerical Analysis Project report NA-81-13, 1981. To appear in SIAM J. Num. Anal., 1982.

[3] P.L. Roe, Approximate Riemann solvers, parameter vectors, and difference schemes, JCP 43(1981), pp. 357–372.

[4] P.L. Roe, Numerical modelling of shock waves and other discontinuities, IMA Conference on Numerical Methods in Computational Aerodynamics, University of Reading, 1981.